Controlled field generation for quad-remeshing

Oliver Schall*
MPI Informatik

Rhaleb Zayer†
MPI Informatik

Hans-Peter Seidel‡
MPI Informatik

Abstract

Quadrangular remeshing of triangulated surfaces has received an increasing attention in recent years. A particularly elegant approach is the extraction of quads from the streamlines of a harmonic field. While the construction of such fields is by now a standard technique in geometry processing, enforcing design constraints is still not fully investigated. This work presents a technique for handling directional constraints by directly controlling the gradient of the field. In this way, line constraints sketched by the user or automatically obtained as feature lines can be fulfilled efficiently. Furthermore, we show the potential of quasi-harmonic fields as a flexible tool for controlling the behavior of the field over the surface. Treating the surface as an inhomogeneous domain we can endow specific surface regions with field attraction/repulsion properties.

CR Categories: I.3.5 [Computer Graphics]: Computational Geometry and Object Modeling—Curve, surface, solid, and object representations; J.6 [Computer Applications]: Computer-Aided Engineering—Computer-aided design

Keywords: quad-remeshing, harmonic fields, quasi-harmonic fields, gradient constraints, conductivity, field control

1 Introduction

Surface meshes delivered by laser scanning technology or iso-surface extraction are in general irregularly sampled which reduces the efficiency of subsequent mesh processing applications. Therefore, conversion into regular triangular or quadrilateral meshes is a common requirement. While triangular meshes are a widespread surface representation, quadrangular meshes are preferable for a considerable number of applications. Their tensor-product nature makes them particularly suited for serving as the parameter domain for spline representations [Li et al. 2006]. Besides computer graphics, other indispensable applications comprise simulations using finite elements or architectural design [Liu et al. 2006; Pottmann et al. 2007]. This stimulated lively research and continuous progress in the areas of quad generation and remeshing.

In this paper, we focus on the design aspects of quad remeshing using vector fields defined over triangular meshes. While the construction of such fields is by now a standard technique in geometry processing, enforcing design constraints is still not fully investigated. This work features the following contributions. First, we present a technique which allows control over the gradient of a harmonic field by aligning it to a set of line constraints. The constraints can be sketched by the user or automatically obtained using a feature line detection algorithm. Furthermore, inspired by the problem of modeling heat flow on inhomogeneous surfaces, we investigate the potential of quasi-harmonic fields as a tool for controlling the behavior of the field over the surface. We demonstrate that it can be used for allowing certain regions on the surface to attract or repulse field contour lines. Both techniques can be used separately or together without affecting the computational cost since the Laplacian is a special case of the quasi-harmonic operator. In all cases the runtime is dominated by solving a single linear system. Additionally, we address issues related to quad construction from the resulting vector fields.

Our approach offers the advantage that no post-processing is needed for resolving clipped primitives as proper alignment is addressed during the field construction stage. Additionally, the tools presented can be seamlessly used in combination with many of the existing quad remeshing techniques [Kälberer et al. 2007; Ray et al. 2006; Tong et al. 2006].

The rest of this paper is organized as follows. An overview of related literature is given in Section (2). Section (3) addresses the construction of gradient constrained harmonic fields and illustrates how quasi-harmonic fields can be used as a tool for field design. The construction of quad meshes is covered in Section (4). Section (5) presents and discusses the results of this work.

2 Related work

In order to fulfill the ever increasing need of quad representations in a wide range of disciplines, research has a productive tradition in the closely related fields of quad-remeshing, parameterization, and vector field design bringing forth a large variety of approaches.

The work of Alliez et al. [2003] on quadrangulation of triangle meshes uses principle curvature directions to guide the remeshing process. This approach was later extended by [Marinov and Kobbelt 2004] to arbitrary meshes by applying curvature line integration on the underlying surface. Dong et al. [2005] compute a harmonic scalar field on the surface and determine the quadrangular facets by tracing integral lines of its gradient and orthogonal co-gradient vector field.

Boier-Martin et al. [2004] employ spatial- and normal-based clustering in order to segment the given triangular mesh into patches from which polygons are computed. Those are subsequently quadrangulated and subdivided resulting in the final quad-mesh. Kharevych et al. [2006] generate a patch layout using circle patterns while [Dong et al. 2006] obtain a segmentation from the Morse-Smale complex of the eigenfunctions of the Laplacian. Marinov and Kobbelt [2006] propose a two-step approach which first segments the mesh using a variant of variational shape approximation [Cohen-Steiner et al. 2004] and then quadrangulates each patch independently using curves with minimum bending energy.

Tong et al. [2006] design quadrangulations by specifying a singularity graph on the triangular mesh. It allows for the representation of line singularities as well as singularities with fractional indices. Based on a modified discrete Laplacian operator, two scalar fields whose iso-contours form the quadrangular mesh are computed. Ray et al. [2006] determine a parameterization of a surface with arbitrary topology by defining two piecewise linear periodic func-

*e-mail: schall@mpi-inf.mpg.de
†e-mail: zayer@mpi-inf.mpg.de
‡e-mail: hpseidel@mpi-inf.mpg.de

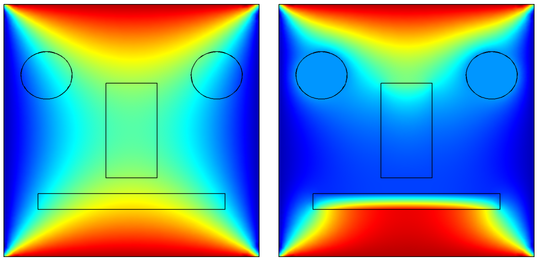

Figure 1: *Heat distribution on a homogeneous (left) and inhomogeneous (right) plate, modeled using the Laplacian operator and the quasi-harmonic operator respectively.*

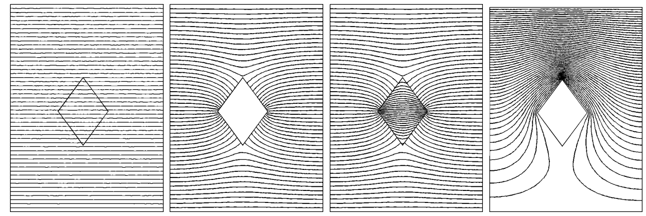

Figure 2: *Contours of quasi-harmonic fields on a rectangular plate. The ratio of conductivity (inversely related to diffusion) between the large and small rectangle was set to 1, 0, 1e-3, 1e3 from left to right respectively. Dirichlet boundary conditions were applied to the top and bottom sides and Neumann boundary conditions to the right and left sides of the plate.*

tions which are aligned with two orthogonal vector fields defined on the surface. The quadrilaterals are subsequently extracted from the bivariate parameterization function. Inspired by this approach, [Kälberer et al. 2007] propose frame fields based on branched covering spaces on a surface. In their context branch points are conceptually similar to singular points with fractional indices. They consider locally integrable fields which are not divergence free to improve the alignment of parameter lines with the given vector field.

Closely related to our approach, Fisher et al. [2007] introduce a technique for the design of tangent vector fields based on discrete exterior calculus which is targeted at designing textures on surfaces. They constrain line integrals of a given vector field over the mesh edges according to a sparse set of user-provided constraints. Unlike their approach which operates on line integrals, we enforce vector constraints directly on the gradient of the field.

3 Constrained fields on surface meshes

In this section, we describe the techniques for controlling the construction of constrained scalar fields on triangular surface meshes. We start from the simple observation that the contours (co-gradient streamlines) of a scalar field are generally easier to construct. Therefore, it seems natural to apply the constraints directly to the contours. Thus the aim is to build harmonic fields whose contours satisfy the design constraints. In order to get a well behaved field on the surface mesh, we require the field to be harmonic. In the present discrete setup this translates to the construction of a piecewise linear function f within each triangle. The construction of such a function amounts to determining its values at the mesh vertices.

In order to control the behavior of the contours, we present two scenarios. The first imposes constraints on the gradient of the harmonic field while the second relies on quasi-harmonic fields which allow for more flexibility in vector field design in comparison to harmonic fields. In both scenarios, the field computation reduces to the solution of a linear system, a task that can be performed efficiently using standard direct or iterative solvers [Davis 2004; Chen et al. 2006].

3.1 Gradient constraints

On a triangular surface mesh, the gradient of a piecewise linear scalar field f is a piecewise constant vector field which exhibits discontinuity on the triangle sides. Analytically, on a triangle T described by its vertices $\{v_1,\ v_2,\ v_3\}$ and of area A and normal n the gradient can be derived as

$$\nabla f \;=\; f_1\,\frac{n\times(v_3-v_2)}{2A} + f_2\,\frac{n\times(v_1-v_3)}{2A} + f_3\,\frac{n\times(v_2-v_1)}{2A}. \tag{1}$$

With this definition in mind, the alignment of contours to line constraints described by the triangle edges they traverse $\{e_i,\ i = 1..n\}$ amounts to imposing the following set of equations on the scalar field f

$$\begin{aligned} \nabla^2 f &= 0 \\ <\nabla f,\, e_i> &= 0\,, i = 1..n, \end{aligned}$$

where $<\cdot,\cdot>$ stands for the dot product. In matrix form, this leads to an augmented matrix consisting of the Laplacian matrix and additional rows representing the gradient constraints. For this linear system to have a unique solution the value of the scalar field needs to be prescribed for at least one vertex.

We note that this approach is independent of the way the line constraints are determined. They can be obtained as feature lines automatically detected using methods such as [Ohtake et al. 2004; Yoshizawa et al. 2005], or defined by the user using a sketching interface. In a preprocessing step, an intermediate mesh which contains new triangles along the feature lines is constructed and all the calculations are performed on it. As the re-triangulation is adaptive w.r.t. the feature lines, the mesh size does not increase significantly. This way our approach is more cost effective in comparison to the construction of higher order fields on the whole surface since elaborate interpolation schemes within the triangulation are avoided.

3.2 Quasi-harmonic fields

While gradient constraints allow to directly enforce field directions by adding additional constraints to the harmonic equation, the approach described in this section allows certain regions to attract or repulse contour lines without introducing additional constraints. For this purpose, we rely on the notion of quasi-harmonic maps [Zayer et al. 2005] to control the behavior of the field contours. The inspiring idea behind the approach stems from simple physical considerations. Let us consider the steady state heat equation on a quadrangular plate. In a first stage, we treat the surface as a homogeneous domain in the sense that the heat conductance is constant over the whole surface. The heat distribution can be obtained by solving a Laplace equation with prescribed conditions. In this example, we apply Dirichlet conditions to the top and bottom sides and Neumann boundary conditions to the right and left sides as illustrated in Figure (1-left).

On the other hand, if we impose specific conductance values for the circular and rectangular sub-domains inside the plate, the standard Laplace equation is not suitable anymore for modeling the heat distribution and we have to rely on the so called quasi-harmonic

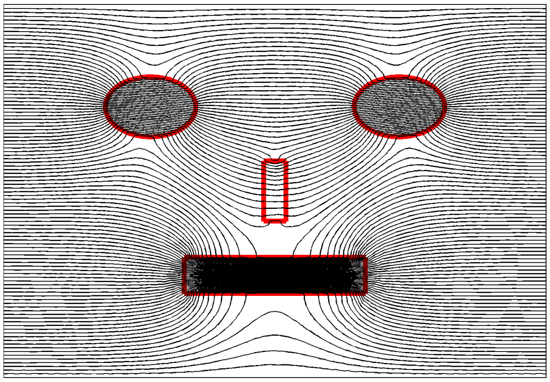

Figure 3: *Contours of a quasi-harmonic field on a rectangular plate. The conductance inside the circular and rectangular regions (red) is several orders of magnitude higher than the plate conductance.*

equation which incorporates the conductance terms, and is therefore sensitive to the inhomogeneous nature of the plate. The heat distribution in this setup is depicted in Figure (1-right).

This example illustrates how simple scalar conductance values can alter the heat distribution on a simple domain. We capitalize on this observation for controlling the behavior of the contour lines.

Our approach proceeds by altering the scalar conductance values C (which are inversely related to diffusion) at the regions of interest and minimizes the following energy functional over the whole surface domain Ω

$$\int_{\Omega} (C\nabla f) \cdot (\nabla f) \ , \tag{2}$$

with prescribed Dirichlet or Neumann boundary conditions. Figures (2) and (3) illustrate the effect of conductance values on the field contour lines. When the conductance is set to 0 on a certain region the field behaves as if Neumann boundary condition were applied at the region boundary. Higher diffusion values make the region repulse the contour lines while lower values make the region attract them.

4 Quad construction

Once the constrained harmonic field has been computed, we use its contours to determine the orientation of the quads. The bottom row of Figure (4) illustrates the work-flow of our quadrangulation algorithm consisting out of two main steps. Firstly, we trace streamlines along and orthogonal to the contours of the harmonic field. In a second step, we use the set of connected streamlines to obtain the final quadrangular mesh.

More precisely, we compute given an harmonic scalar value at every vertex of the triangular mesh, the piecewise constant gradient on each triangle using the gradient discretization provided in equation (1). As it is usually desirable to have quads as rectangular as possible, we also determine the vector field orthogonal to the gradient vectors on each triangle which will be denoted in the following as co-gradient field. The co-gradient field is computed as the vector product of the gradient vector and the triangle normal on each face of the mesh. In specific situations the placement of line constraints may lead to a configuration where two edges of a triangle are constrained. A special treatment consisting of targeted subdivisions of the affected faces yields a correct behavior as illustrated in Figure (5).

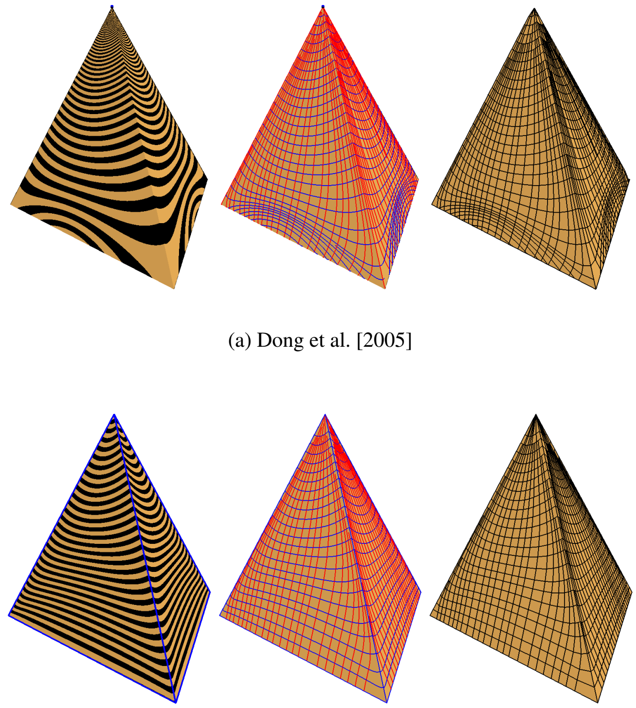

(a) Dong et al. [2005]

(b) our approach

Figure 4: *Comparison between the approach introduced by Dong et al. [2005] (a) and our technique (b). The textured models (left column) illustrate the behavior of the contours of the harmonic fields for both techniques. For our approach the gradient is constrained orthogonal to the ascending edges and tangential to the base edges of the tetrahedron. This way, we avoid clipped primitives and obtain a proper alignment of the quads (right column) to the features of the surface.*

We regard a streamline as a piecewise linear curve on the surface which integrates one of the tangential vector fields and whose vertices are located on the edges of the triangular mesh. Starting from a given seed point, the streamline is integrated in the positive and negative field direction until it either creates a loop, approaches another streamline too closely or meets a singularity.

The singularities in the gradient vector field are detected based on the definition of the index of a critical point. Consider a continuous vector field V and a closed curve γ. Suppose that there are no critical points of V on γ. Let us move a point P along the curve in the counterclockwise direction. The vector $V(P)$ will rotate during the motion. When P returns to its starting place after one revolution along the curve, $V(P)$ also returns to its original position. During the journey $V(P)$ will make some whole number of revolutions. Counting these revolutions positively if they are counterclockwise, negatively if they are clockwise, the resulting algebraic sum of the number of revolutions is called the winding number of V on γ. The index of a point in the vector field V is then defined as the winding number of a small counterclockwise oriented circle centered at that point. A discretization of this definition for piecewise linear vector fields on surfaces is introduced in [Ray et al. 2007]. We use a simplified version of their formulations which allows us to compute the

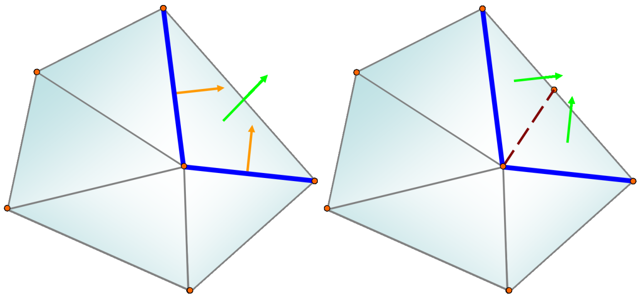

Figure 5: *In the special case where a line constraint (bold blue lines) covers two edges of one triangle, the gradient vector on the triangle (green) cannot be aligned to both vector constraint (orange) simultaneously. This is remedied by half-splitting the triangle as shown in the image to the right.*

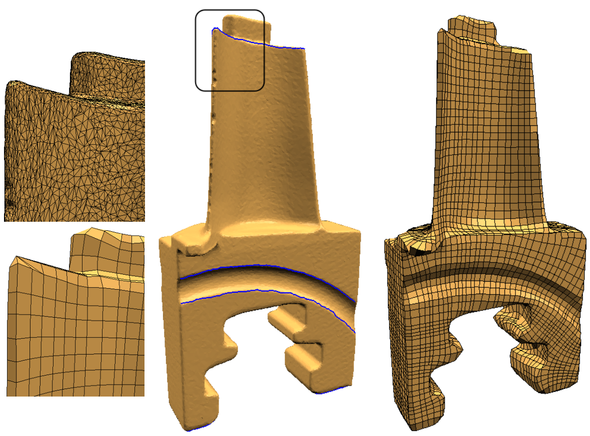

(a) (b) (c)

Figure 6: *Remeshing of a reconstructed laser-scanned Turbine Blade model with irregular triangulation. The remeshing process is guided by gradient constraints indicated by the blue lines (b). The remeshed result (c) as well as the zooms (a) show that the quads are properly aligned along the blade as well as the selected prominent features.*

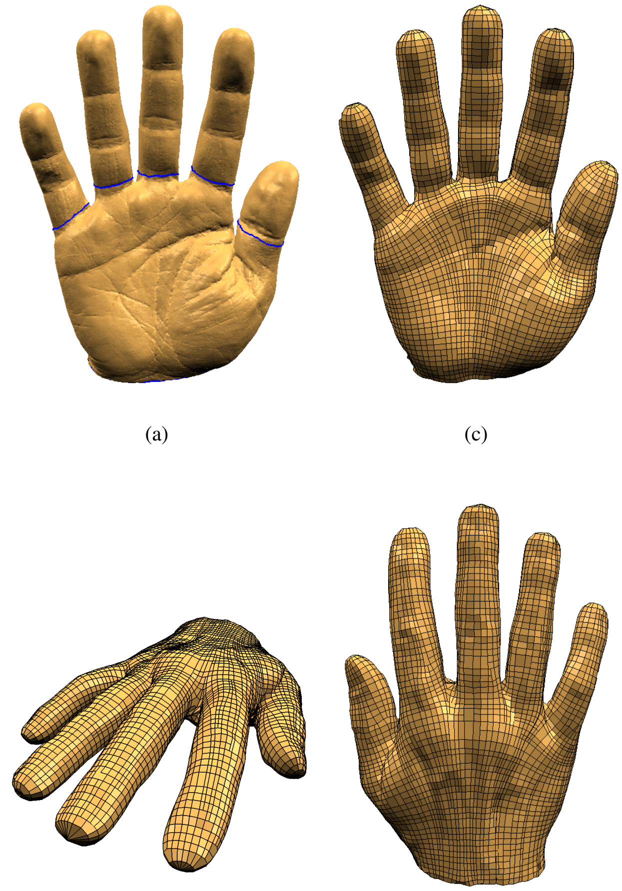

(a) (c) (b) (d)

Figure 7: *The laser-scanned hand model is remeshed guided by gradient constraints (a) which permits the resulting quads to follow the shape of the hand in an intuitive manner (c)+(d). Furthermore, our approach automatically places the singularities at the fingertips properly although the constraints are chosen very distant to them (b).*

index at a vertex v of our gradient vector field as

$$I(v) = \frac{1}{2\pi} \sum_{e \in \mathcal{N}(v)} \Theta(e) + A_d(v) \tag{3}$$

where $A_d(v)$ is the angle deficit at v and $\Theta(e)$ is the angle between the gradient vectors $\vec{g}(t_0)$ and $\vec{g}(t_1)$ after flattening the pair of triangles t_0 and t_1 adjacent to the edge e. We thus determine the extremal vertices as well as the saddle points as the points with the index 1 and -1, respectively.

In order to trace streamlines on the surface, we sample the line constraints regularly and choose the selected points as seeds for the gradient streamlines. To cover the whole mesh we also place seed points on both sides of the streamline while it is traced according to a user-defined distance measure which controls the quad size. The co-gradient streamlines are traced accordingly by propagating them over the surface starting from the line constraints.

In the second step, we reconstruct quads from the set of streamlines. For this, we first determine the intersection points of gradient and co-gradient streamlines. In order to perform this efficiently, we associate the line segments of all streamlines with the triangles they are integrated on and compute the intersections on all triangles. This way, we obtain a graph of streamlines which are interconnected at their intersection points. Starting at these intersections we traverse the graph to create the quadrangular faces.

5 Results and Discussion

We tested our approach on a benchmark of triangular meshes covering synthetic and reconstructed laser-scanned data. Typical results are featured in Figure (4) and Figures (6)-(8).

A comparison to the clipping approach used in [Dong et al. 2005], on a tetrahedron model reveals that our approach handles sharp features in an accurate manner as the alignment to line constraints is performed during the field computation (see Figure (4)).

Figures (6)+(7) illustrate remeshing results of our approach on ir-

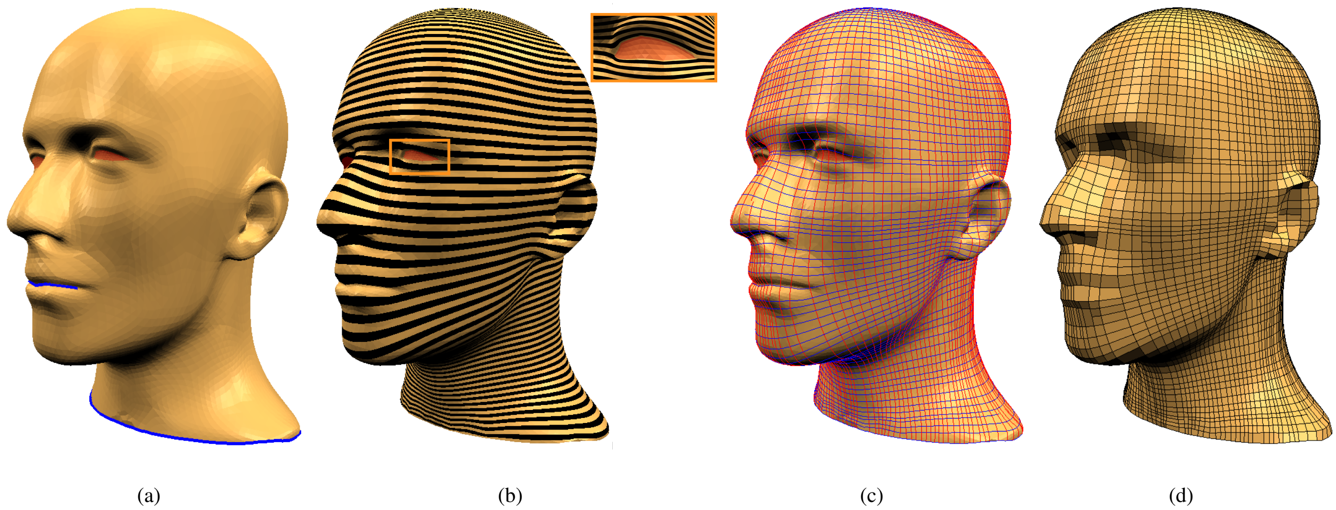

Figure 8: *Remeshing of the mannequin model using areas with modified conductivity (red regions) and gradient constraints (blue lines). The variation in the conductivity creates a repulsive effect such that the contour lines of the harmonic field (b) and thus the streamlines (c) bend around the eye region resulting in a special consideration of this surface part in the final quadrangular remeshing (d). Note that the gradient constraints specified at the lips as well as the neck ensure a proper quad alignment.*

regularly sampled data reconstructed from laser scans. While line constraints are useful to align quads to important features of the surface as illustrated on the Turbine Blade model, they can be further used to guide streamlines along user-specified constraints. The resulting remesh of the hand model reflects that the quads intuitively align to the shape of the surface.

In Figure (8) we apply quasi-harmonic fields for driving the remeshing process. Using higher conductivity, contours around the eye region are repelled which allows the generated quads to follow the natural shape of the eyes.

Our approach is fast as the runtime is dominated by the solution of a linear system which can be solved efficiently using direct or iterative solvers. Even for large meshes such as the hand model consisting out of nearly 400K triangles runtimes are in the order of seconds. The subsequent streamline tracing as well as the quad generation is performed in only a few seconds.

As our approach enforces directional constraints it may introduce additional singularities especially when certain line constraints form a closed curve. Those can be found efficiently during streamline tracing using the singularity detection technique described earlier. We do not see this as a limitation of our approach as it can be used to place new singularities at desired locations for design purposes such as the fingertips of the hand model illustrated in Figure (7).

6 Conclusion

In this paper, we presented a set of flexible and versatile tools for designing scalar fields on surfaces. Two scenarios for controlling the field behavior on the surface are demonstrated. By operating directly on the gradient of the scalar field our technique can enforce directional constraints which makes it suitable for avoiding tedious post processing, generally needed for aligning quads to important features. Regarding a surface as an inhomogeneous domain, we introduced quasi-harmonic fields as a design tool which endows surface regions with attraction/repulsion properties. This makes it a more general and flexible design tool in comparison to standard harmonic fields. These techniques can be used independently or on top of existing field-based quad-remeshing methods. The substantiated results demonstrate the quality of our quad-remeshing approach and confirms the flexibility of our field construction techniques.

Acknowledgements

We would like to thank the anonymous reviewers for their helpful comments and suggestions. The Blade and Hand datasets are courtesy of the AIM@SHAPE Shape Repository. This work was supported in part by the European FP6 NoE grant 506766 (AIM@SHAPE).

References

ALLIEZ, P., COHEN-STEINER, D., DEVILLERS, O., LÉVY, B., AND DESBRUN, M. 2003. Anisotropic polygonal remeshing. *ACM Transactions on Graphics 22*, 3, 485–493. Proceedings of ACM SIGGRAPH 2003.

BOIER-MARTIN, I., RUSHMEIER, H., AND JIN, J. 2004. Parameterization of triangle meshes over quadrilateral domains. In *Eurographics/ACM SIGGRAPH Symposium on Geometry Processing 2004*, ACM, New York, NY, USA, 193–203.

CHEN, Y., DAVIS, T. A., HAGER, W. W., AND RAJAMANICKAM, S. 2006. Algorithm 8xx: Cholmod, supernodal sparse cholesky factorization and update/downdate. Tech. Rep. TR-2006-005. submitted to ACM Transactions on Mathematical Software.

COHEN-STEINER, D., ALLIEZ, P., AND DESBRUN, M. 2004. Variational shape approximation. *ACM Transactions on Graphics 23*, 3, 905–914. Proceedings of ACM SIGGRAPH 2004.

DAVIS, T. A. 2004. Algorithm 832: Umfpack, an unsymmetric-pattern multifrontal method. *ACM Transactions on Mathematical Software 30*, 2 (June), 196–199.

DONG, S., KIRCHER, S., AND GARLAND, M. 2005. Harmonic functions for quadrilateral remeshing of arbitrary manifolds. *Computer-Aided Design 22*, 4, 392–423.

DONG, S., BREMER, P.-T., GARLAND, M., PASCUCCI, V., AND HART, J. C. 2006. Spectral surface quadrangulation. *ACM Transactions on Graphics 25*, 3, 1057–1066. Proceedings of ACM SIGGRAPH 2006.

FISHER, M., SCHRÖDER, P., DESBRUN, M., AND HOPPE, H. 2007. Design of tangent vector fields. *ACM Transactions on Graphics 26*, 3, 56. Proceedings of ACM SIGGRAPH 2007.

KÄLBERER, F., NIESER, M., AND POLTHIER, K. 2007. Quad-Cover - surface parameterization using branched coverings. *Computer Graphics Forum 26*, 3, 375–384.

KHAREVYCH, L., SPRINGBORN, B., AND SCHRÖDER, P. 2006. Discrete conformal mappings via circle patterns. *ACM Transactions on Graphics 25*, 2, 412–438.

LI, W.-C., RAY, N., AND LÉVY, B. 2006. Automatic and interactive mesh to T-spline conversion. In *Eurographics/ACM SIGGRAPH Symposium on Geometry Processing 2006*, 191–200.

LIU, Y., POTTMANN, H., WALLNER, J., YANG, Y.-L., AND WANG, W. 2006. Geometric modeling with conical meshes and developable surfaces. *ACM Transactions on Graphics 25*, 3, 681–689. Proceedings of ACM SIGGRAPH 2006.

MARINOV, M., AND KOBBELT, L. 2004. Direct anisotropic quad-dominant remeshing. In *Proc. of the 12th Pacific Conf. on Comp. Graph. and Appl.*, 207–216.

MARINOV, M., AND KOBBELT, L. 2006. A robust two-step procedure for quad-dominant remeshing. *Computer Graphics Forum 25*, 3, 207–216.

OHTAKE, Y., BELYAEV, A., AND SEIDEL, H.-P. 2004. Ridge-valley lines on meshes via implicit surface fitting. *ACM Transactions on Graphics 23*, 3, 609–612. Proceedings of ACM SIGGRAPH 2004.

POTTMANN, H., LIU, Y., WALLNER, J., BOBENKO, A., AND WANG, W. 2007. Geometry of multi-layer freeform structures for architecture. *ACM Transactions on Graphics 26*, 3, 65. Proceedings of ACM SIGGRAPH 2007.

RAY, N., W.-C., L., LÉVY, B., SHEFFER, A., AND ALLIEZ, P. 2006. Periodic global parameterization. *ACM Transactions on Graphics 25*, 4, 1460–1485.

RAY, N., VALLET, B., LI, W.-C., AND LÉVY, B. 2007. N-symmetry direction field design. *ACM Transactions on Graphics*. accepted pending revisions, to appear.

TONG, Y., ALLIEZ, P., COHEN-STEINER, D., AND DESBRUN, M. 2006. Designing quadrangulations with discrete harmonic forms. In *Eurographics/ACM SIGGRAPH Symposium on Geometry Processing 2006*, 201–210.

YOSHIZAWA, S., BELYAEV, A., AND SEIDEL, H.-P. 2005. Fast and robust detection of crest lines on meshes. In *ACM Symposium on Solid and Physical modeling 2005*, ACM, New York, NY, USA, 227–232.

ZAYER, R., RÖSSL, C., AND SEIDEL, H.-P. 2005. Discrete tensorial quasi-harmonic maps. In *Shape Modeling International 2005 (SMI 2005)*, 276–285.